

Density-Functional Study of Structural and Electronic Properties of the $Zr_nAl^{\pm m}$ Clusters

Jun-Zai Yu¹, Feng-Qi Zhao², Si-Yu Xu², Lu-Jing Sun³, Xue-Hai Ju¹

¹Key Laboratory of Soft Chemistry and Functional Materials of MOE, School of Chemical Engineering, Nanjing University of Science and Technology, Nanjing 210094, P. R. China

²Laboratory of Science and Technology on Combustion and Explosion, Xi'an Modern Chemistry Research Institute, Xi'an 710065, P. R. China

³School of Chemistry and Materials Science, Nanjing Normal University, Nanjing 210094, P. R. China

Correspondence: Xue-Hai Ju, School of Chemical Engineering, Nanjing University of Science and Technology, Nanjing, P. R. China. E-mail: xhju@njust.edu.cn

Received: September 22, 2016 Accepted: October 10, 2016 Online Published: October 13, 2016

doi:10.5539/ijc.v8n4p111

URL: <http://dx.doi.org/10.5539/ijc.v8n4p111>

Abstract

The geometries, stabilities, and electronic properties of $Zr_nAl^{\pm m}$ ($n = 1 - 7$ and $m = 0, 1$) clusters were investigated at the UB3LYP/LANL2DZ level. The variations of structural and electronic properties with the changes of n and m were probed. Several possible multiplicities of each cluster were tested. The multiplicity of the most stable neutral clusters is 4 instead of 2. For all the three differently charged of Zr_nAl clusters, the lowest-energy geometry is in favor of three-dimensional structure when $n \geq 3$. The Zr_3Al^+ , Zr_4Al^- , Zr_5Al^+ , Zr_6Al^- and Zr_7Al clusters are more stable than their corresponding differently charged species of the same size. Moreover, the odd-even oscillations are found in the fragmentation energy and the second-order difference of total energies for Zr_nAl^- clusters. The Zr_2Al^+ cluster is more inert to chemical reaction than others judged by the HOMO-LUMO gaps. NBO analysis was done to analysis the electronic properties.

Keywords: $Zr_nAl^{\pm m}$ clusters, UB3LYP/LANL2DZ, odd-even oscillations, NBO, three-dimensional structures

1. Introduction

Recently, a large number of experimental and theoretical studies of clusters were performed (Alexandrova et al, 2004), (Zhai et al, 2003), (Lei, 2011), (Hua et al, 2013), (Addicoat et al, 2007), because they have many unique physical and chemical properties in the terms of the geometry and electronic properties (Schmidt et al, 1998), (Herry, 2012), but also have potential applications in catalysis (Yamazoe et al, 2014), (Tang et al, 2014), hydrogen storage (Ramos-Castillo et al, 2015), (Wu et al, 2015) etc. Moreover, the study of clusters plays a key role in understanding the growth behavior of microscopic particles of their bulk.

As we all know, zirconium atom is a rare metal, a $4d$ transition-metal (TM), and has an electronic configuration of $4d^25s^2$. The Zr material used in the nuclear industry for cladding fuel elements, and own to a lower absorption cross section for neutrons. It is very resistant to corrosion by many common acids, alkalis, and sea water. Therefore, the metal, which is utilized as an alloying agent in steel and for making surgical appliances, is developed extensively by the chemical industry where corrosive agents are employed (Zhao et al, 2009), (Wang, 2006). Due to these special properties of TM Zr clusters, a number of research groups have been striving to investigate the geometrical structures and electronic properties for X-doped ($X =$ metals) zirconium and the pure zirconium clusters recently. (Zhao et al, 2009), (Wang, 2006), (Sengupta et al, 2016), (Yang et al, 2008). (Lekka, 2010) investigated the bonding characteristics and mechanical properties of Cu-Zr and Cu-Zr-Al clusters by density functional theory (DFT), they found the most abundant microstructural units on the $Cu_{60}Zr_{40}$ cluster. Zhao and co-workers studied the structural, electronic, and magnetic properties of the Zr_nCr ($n = 2-14$) clusters, showed that the Zr_6Cr , Zr_8Cr and $Zr_{12}Cr$ clusters are more stable than their neighbors. (Zhao et al, 2009). The chemisorption of molecular hydrogen on small Zr_n clusters ($n = 2-15$) was performed by (Sheng et al, 2008). The preferred adsorption sites for H_2 reacting with the Zr_n clusters are the bridge sites. As for Al-doped Zr clusters, (Du et al, 2010) were studied the geometrical and electronic properties of neutral $Zr_{n-1}Al$ clusters and the pure Zr_n clusters ($n = 2-8$) with hybrid HF/DFT functional. From the above reports, although there are a lot of researches for X-doped Zr clusters, but few researches are systematically performed for the neutral and

positively/negatively charged Al-doped zirconium clusters. What is the difference between the neutral Zr_nAl and Zr_nAl^{\pm} clusters? Can we find the "odd-even alteration" phenomenon in $Zr_nAl^{\pm m}$ clusters as in MgB_n clusters (Wu et al, 2014) for some properties? To explore these, we investigated the geometric structures, stabilities and electronic properties of $Zr_nAl^{\pm m}$ ($n = 1-7$ and $m = 0, 1$) clusters.

2. Computational Methods

All the clusters were optimized by the B3LYP method (Lee et al, 1988), (Becke, 1993) in combination with the LANL2DZ basis set (Hay & Wadt, 1985). This basis set is modified by the relativistic effective core potential, therefore, is suitable for the transition metals (TM) Zr clusters (Yao et al, 2008), (Ge et al, 2012). In order to check the correctness of this method used for the investigation of the Zr_nAl clusters, we first accomplished the calculation on Al_2 and Zr_2 dimers. The bond length of the Al_2 (2.64 Å) and Zr_2 (2.33 Å) dimers are in nice accordance with experimental value of 2.70 Å (Fu et al, 1990) and 2.24 Å (Doverstål et al, 1998), respectively.

We have also considered the spin multiplicities for the initial configurations of $Zr_nAl^{\pm m}$ clusters ($n = 1 - 7$ and $m = 0, 1$). To investigate the relative stability of differently charged Zr_nAl clusters, we calculated the average binding energy, fragmentation energy and the second-order difference in total energies. The average binding energy (E_b) for $Al_{13}B_n$ clusters can be defined by the following formula:

$$E_b(n)^{\pm m} = [nE(Zr) + E(Al)^{\pm m} - E(Zr_nAl)^{\pm m}]/(n + 1) \quad (1)$$

The fragmentation energy (E_f) can be defined by the following formula:

$$E_f(n)^{\pm m} = E(Zr) + E(Zr_{n-1}Al)^{\pm m} - E(Zr_nAl)^{\pm m} \quad (2)$$

The second-order difference of total energies (Δ_2E) can be defined by the following formula:

$$\Delta_2E(n)^{\pm m} = E(Zr_{n+1}Al)^{\pm m} + E(Zr_{n-1}Al)^{\pm m} - 2E(Zr_nAl)^{\pm m} \quad (3)$$

where $E(Zr_{n+1}Al)^{\pm m}$, $E(Zr_{n-1}Al)^{\pm m}$ and $E(Zr_nAl)^{\pm m}$ represent the energies of the most stable of $Zr_{n+1}Al^{\pm m}$, $Zr_{n-1}Al^{\pm m}$ and $Zr_nAl^{\pm m}$ clusters, respectively. $E(Zr)$ and $E(Al)^{\pm m}$ represent the total energies of the Zr and $Al^{\pm m}$ atoms, respectively. For the electronic properties, we calculated HOMO-LUMO (highest occupied molecular orbital-lowest unoccupied molecular orbital) gaps energies and the chemical hardness for the most stable $Zr_nAl^{\pm m}$ clusters. Chemical hardness is defined as the resistance of chemical potential to a change in the number of electrons: (Pearson, 2005), (Suh et al, 2015)

$$\eta = (I - A)/2 \quad (4)$$

where I and A are the ionization potential and electron affinity, respectively.

The natural bond orbital (NBO) (Carpenter & Weinhold, 1988), (Reed et al, 1988) analysis was carried out for the most stable structures in order to study the chemical bonding characteristics. All the computations were performed through Gaussian 09 package (Frisch et al, 2010).

3. Results and Discussion

3.1 Stable Geometric Structure

The fully optimized structures with lowest-energy and low-lying metastable isomers of $Zr_nAl^{\pm m}$ clusters were shown in Figure 1. Through this figure we can fully understand the characteristics of different charged Zr_nAl clusters enough. For $n = 2$, the lowest-energy structures of $AlZr_2$ and $AlZr_2^-$ are isosceles triangle (C_{2v}), whose apex angle (Zr-Al-Zr) are 50.26° and 53.75° , respectively, and the Al-Zr bond length are slightly different (See Table 1). While the most stable structure of Zr_2Al^+ cluster is a chain, the energy of Zr_2Al^+ cluster is 0.09 eV lower than its isosceles triangle structure. This phenomenon of structures for $Zr_2Al^{\pm m}$ clusters is similar to $B_2Mg^{\pm m}$ clusters (Wu et al, 2014). As for $Zr_3Al^{\pm m}$ clusters, we got the distorted tetrahedron geometry (3a) with C_1 symmetry for Zr_3Al cluster, but the lowest-energy structures of Zr_3Al^{\pm} clusters are trigonal pyramid with C_{2v} symmetry. The second most stable structure for the cation Zr_3Al^+ cluster is a quadrilateral structure with C_{2v} symmetry whose total energy is 1.04 eV higher than the lowest-energy structure. We also tried to construct some planar and quasi-planar structures as initial configuration, but these initial configurations change to the three-dimensional (3D) structures for Zr_3Al and Zr_3Al^- clusters during the geometrical optimization. The V-like structures appear in Zr_3Al and Zr_3Al^- clusters, whose energy are 0.11 eV and 0.36 eV larger than the most stable ones, respectively.

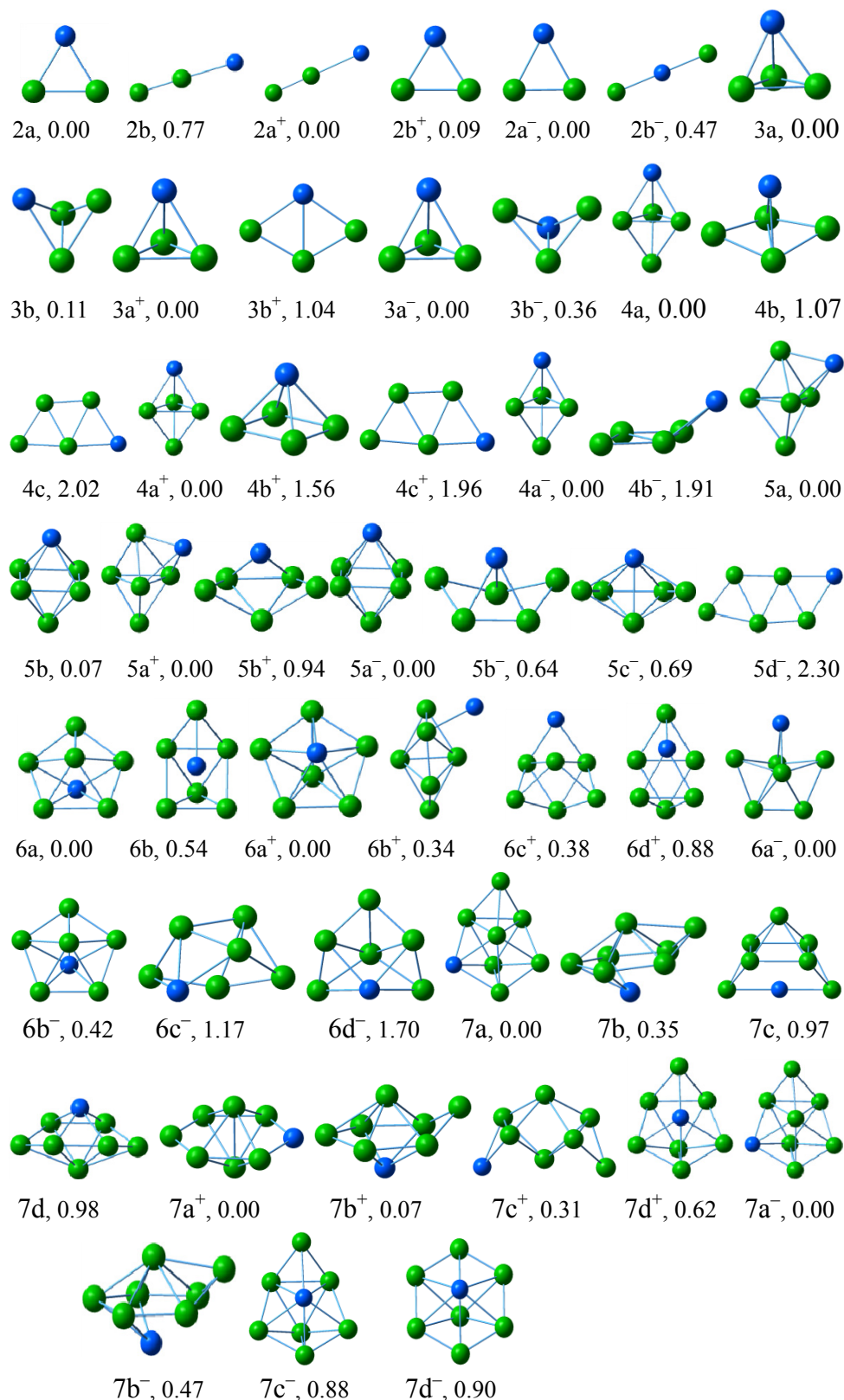


Figure 1. Lowest-energy and low-lying structures of Zr_nAl^m ($n = 1 - 7$ and $m = 0, 1$) clusters. (The first digit denotes the number of zirconium, the letter (a, b, c, d) is the structure label (from lower to higher energy), superscript + or - denotes a positive/negative charge, and the 0.00 represents the relative energy in eV. Others are similar)

Table 1. Shortest Zr-Al bond lengths ($R_{\text{Zr-Al, min}}$), shortest Zr-Zr bond lengths ($R_{\text{Zr-Zr, min}}$), average Zr-Zr bond lengths ($R_{\text{Zr-Zr, ave}}$), multiplicity, symmetry and electronic state of the $\text{Zr}_n\text{Al}^{\pm m}$ ($n = 1 - 7$, $m = 0, 1$) clusters for the lowest-energy structures^a

Cluster	Multi.	Symmetry	$R_{\text{Al-Zr, min}}$	$R_{\text{Zr-Zr, min}}$	$R_{\text{Zr-Zr, ave}}$
AlZr	4	$D_{\infty h}$	2.58	—	—
AlZr ₂	4	C_{2v}	2.88	2.45	2.45
AlZr ₃	4	C_1	2.73	2.63	2.76
AlZr ₄	4	C_{3v}	2.83	2.79	2.82
AlZr ₅	4	C_s	2.74	2.76	2.87
AlZr ₆	4	C_s	2.76	2.72	2.84
AlZr ₇	4	C_1	2.85	2.74	2.87
AlZr ⁺	1	$D_{\infty h}$	2.42	—	—
AlZr ₂ ⁺	1	$D_{\infty h}$	3.07	2.30	2.30
AlZr ₃ ⁺	3	C_{3v}	2.78	2.77	2.78
AlZr ₄ ⁺	3	C_{3v}	2.83	2.79	2.85
AlZr ₅ ⁺	3	C_1	2.79	2.74	2.87
AlZr ₆ ⁺	3	C_s	2.82	2.86	2.88
AlZr ₇ ⁺	1	C_{2v}	2.71	2.61	2.71
AlZr ⁻	3	$D_{\infty h}$	2.67	—	—
AlZr ₂ ⁻	3	C_{2v}	2.79	2.52	2.52
AlZr ₃ ⁻	1	C_{3v}	2.85	2.75	2.75
AlZr ₄ ⁻	3	C_{3v}	2.84	2.82	2.82
AlZr ₅ ⁻	1	C_{4v}	2.93	2.79	2.79
AlZr ₆ ⁻	1	C_{2v}	2.83	2.60	2.60
AlZr ₇ ⁻	1	C_1	2.85	2.66	2.86

^a Bond lengths in Å.

The $\text{Zr}_4\text{Al}^{\pm m}$ clusters favor trigonal bipyramid (TBP) structures with C_{3v} symmetry ($4a$, $4a^+$, $4a^-$) as the lowest-energy structures. It is noteworthy that there is a tetragonal pyramid isomer ($4b^+$) with high C_{4v} symmetry, but the relative energy (ΔE) is 1.56 eV. The most stable structures for Zr_5Al and Zr_5Al^+ clusters are in 3D configurations (similar to Al-capped add the top right of TBP structure), and with high spin multiplicity and C_1 symmetry. Meanwhile, the minimum Al-Zr bond lengths are 2.74 Å and 2.79 Å for Zr_5Al and Zr_5Al^+ clusters, respectively. For Zr_5Al^- cluster, the most stable structures is a rectangular bipyramid with the Al atom located at an apex of the bipyramid ($5a^-$, C_{4v}). As for $n = 6$ and 7, we have optimized the isomers for $\text{Zr}_6\text{Al}^{\pm m}$ and $\text{Zr}_7\text{Al}^{\pm m}$ clusters, all the stable structures are 3D geometry. This phenomenon has also been found for AlB_n clusters. (Feng & Luo, 2007)

3.2 Relative Stability

We plotted the binding energies (E_b) for the most stable structures of $\text{Zr}_n\text{Al}^{\pm m}$ clusters in Figure 2, The E_b generally increases with increasing cluster size. No odd-even oscillations are exhibited. As a whole, the average binding energies of the Zr_nAl clusters are smaller than those of the Zr_nAl^+ and Zr_nAl^- clusters from $n \geq 2$, indicating that the Zr_nAl clusters gain stability after the gain or loss of one electron, this phenomenon is similar to $\text{MgB}_n^{\pm m}$ clusters (Wu et al, 2014). It can be observed that the E_b essentially increases sharply when n goes from 1 to 4, but increasing smoothly when $n \geq 4$.

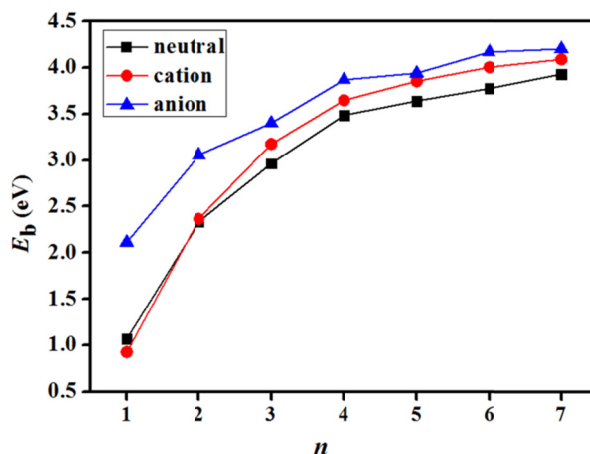


Figure 2. Clusters size (n) dependence of the average binding energy (E_b) of $\text{Zr}_n\text{Al}^{\pm m}$ clusters

As show in Figure 3, the fragmentation energies (E_f) for the anionic Zr_nAl clusters have an obvious odd-even oscillation with increasing size of clusters. The local maximum fragmentation energies appear at $n = 4$ and 6 for the anionic Zr_nAl clusters, indicating that $AlZr_4^-$ and $AlZr_6^-$ clusters are more stable than their neighbors of Zr_nAl^- clusters. The local minimum E_f appears at Zr_5Al , Zr_5Al^- and Zr_7Al^+ clusters, it means that these clusters are less stable than their neighbors.

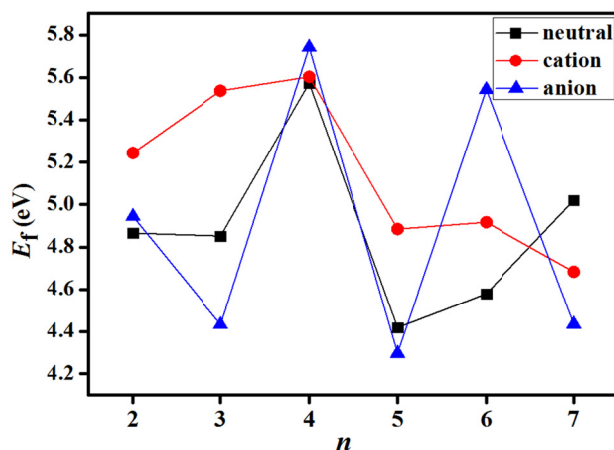


Figure 3. Cluster size (n) dependence of the fragmentation energy (E_f) for $Zr_nAl^{\pm m}$ clusters

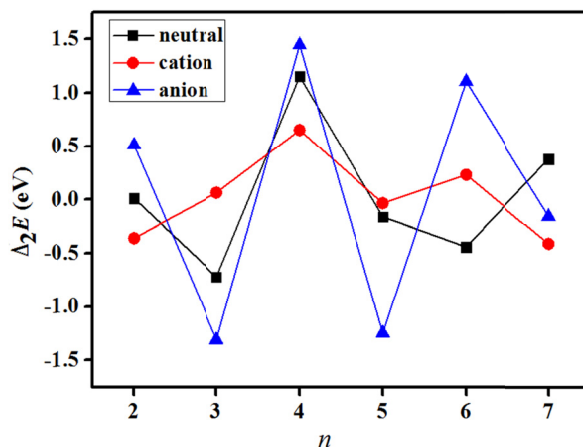


Figure 4. Cluster size (n) dependence of the second-order difference energy (Δ_2E) for $Zr_nAl^{\pm m}$ clusters

There is a sensitive quantity that can reflect the relative stability of clusters (Wang et al, 2010), this parameter is the second-order difference of total energies (Δ_2E) in Figure 4 and it was calculated with Eq. (3). The values of Δ_2E are the largest at $n = 4$ for all three kinds of clusters, indicating that these clusters present the highest stabilities with respect to the clusters with the same charge. This is probably due to the $Zr_4Al^{\pm m}$ clusters having high symmetry (C_{3v}) and more charge transfer from Zr atoms to Al atom (Table 2). This viewpoint could be partially supported by Ref (Feng & Luo, 2007). Additionally, we analyzed the relationship among different charged clusters in Figure 4. The second-order difference of total energies of Zr_3Al^+ , Zr_4Al^- , Zr_5Al^+ , Zr_6Al^- and Zr_7Al clusters are larger than their corresponding species, this phenomenon also appears in Figure 3.

3.3 Electronic Property

The HOMO-LUMO gap (G_{HL}) is the prototypical electronic property and is an invaluable parameter in clusters electronic property analysis. (Du et al, 2010). Therefore, we have calculated the G_{HL} of $Zr_nAl^{\pm m}$ clusters in Figure 5. The G_{HL} values of the cationic Zr_nAl clusters are usually larger than those of neutral and anionic Zr_nAl clusters except at $n = 4$ and 7 , and the gaps are close to each other at $n = 5$ and 7 within 0.072eV and 0.030eV . It should be pointed out that the gaps of all clusters have minimum and maximum values for $ZrAl$ and Zr_2Al^+ , respectively, indicating that the $ZrAl$ cluster has the highest chemical activities, but the Zr_2Al^+ cluster is the most inert in $Zr_nAl^{\pm m}$ clusters. In this figure, we found no correlation between the HOMO-LUMO gaps and the energetic stability of these clusters. (Feng & Luo, 2007)

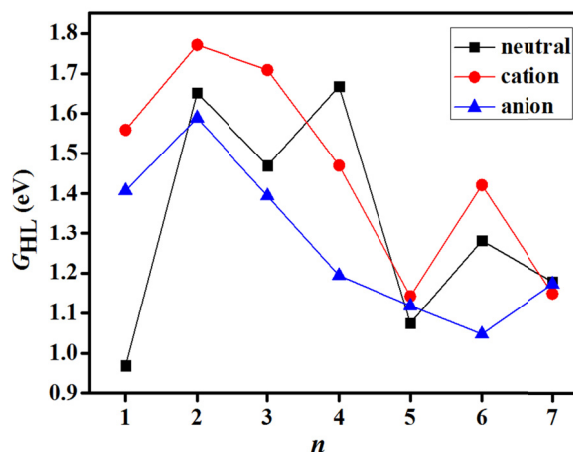


Figure 5. Cluster size (n) dependence of HOMO-LUMO gaps (G_{HL}) energy for $Zr_n Al^{\pm m}$ clusters

We calculated the chemical hardness (η) for neutral $Zr_n Al$ clusters and the results are displayed in Figure 6. The maximum hardness principle can be understood from eq 4. Bigger η means larger ionization potential and smaller electron affinity, which implies that the system has a smaller tendency to accept electrons and/or a smaller tendency to give away electrons. (Parr & Zhou, 1993). As can be seen in Figure 6, the trend of η is decreasing with the increase of size from $n = 2$ to 6, it means that the neutral $Zr_n Al$ clusters have a larger tendency to accept or give away electrons as the clusters size increases.

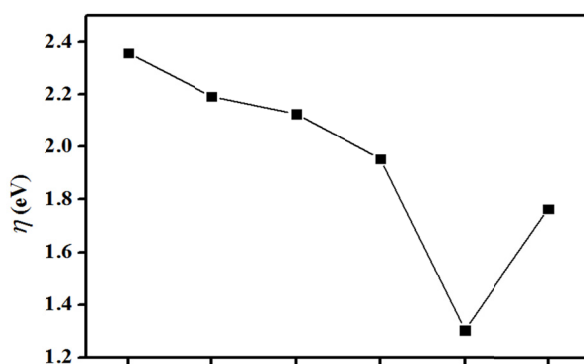


Figure 6. Cluster size (n) dependence of chemical hardness (η) for neutral $Zr_n Al$ clusters

The NBO method provides an effective electronic configuration for each atom in a cluster owing to the localized orbital constructed from the occupancy-weighted symmetric orthogonalized natural atomic orbital (Wu et al, 2009). Therefore, we studied the atomic charges (Q_{Al}) of Al atom versus the size n of clusters in Figure 7 and the natural electron configuration of Al atom was listed in Table 2. $Zr_4 Al$, $Zr_4 Al^+$ and $Zr_4 Al^-$ clusters are chosen as examples. The values of Q_{Al} for $Zr_4 Al^{\pm m}$ clusters are negative, indicating that the charges transfer from Zr atoms to Al atom. On the contrary, charges in other clusters transfer from Al atom to Zr atoms. This could be further demonstrated by the natural electron configuration of Al atom being $3s^{0.76}3p^{0.74}$, $3s^{0.79}3p^{0.74}$ and $3s^{0.74}3p^{0.81}$ for $Zr_4 Al$, $Zr_4 Al^+$ and $Zr_4 Al^-$ clusters, respectively. Therefore, the electrostatic interaction between the Al atom and Zr atoms of the $Zr_4 Al^{\pm m}$ clusters are stronger than that of other clusters, indicating that the $Zr_4 Al^{\pm m}$ clusters are more stable than other clusters. (Feng & Luo, 2007)

Table 2. The natural electron configuration of Al atom in $Zr_n Al^{\pm m}$ ($n = 1 - 7, m = 0, 1$) clusters

n	neutral	cation	anion
1	$3s^{0.8}43p^{0.42}$	$3s^{0.85}3p^{0.37}$	$3s^{0.90}3p^{0.67}$
2	$3s^{0.86}3p^{0.26}$	$3s^{0.96}3p^{0.23}$	$3s^{0.81}3p^{0.68}$
3	$3s^{0.76}3p^{0.69}$	$3s^{0.75}3p^{0.63}$	$3s^{0.74}3p^{0.78}$
4	$3s^{0.76}3p^{0.74}$	$3s^{0.79}3p^{0.74}$	$3s^{0.74}3p^{0.81}$
5	$3s^{0.70}3p^{0.61}$	$3s^{0.72}3p^{0.52}$	$3s^{0.68}3p^{0.73}$
6	$3s^{0.52}3p^{0.86}$	$3s^{0.53}3p^{0.80}$	$3s^{0.65}3p^{0.72}$
7	$3s^{0.62}3p^{0.69}$	$3s^{0.61}3p^{0.69}$	$3s^{0.63}3p^{0.70}$

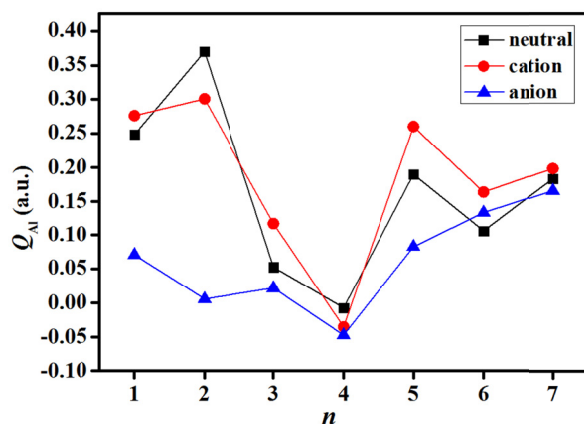


Figure 7. Cluster size (n) dependence of average atomic charges (Q_{Al}) of Al in $Zr_nAl^{\pm m}$ clusters

4. Conclusions

The geometries, relative stability and electronic property of the $Zr_nAl^{\pm m}$ clusters were investigated at the B3LYP/LANL2DZ level. For $Zr_6Al^{\pm m}$ clusters and $Zr_7Al^{\pm m}$ clusters, all stable structures are three-dimensional. The average binding energies of $Zr_nAl^{\pm m}$ clusters increase as the size n increases. It is noticeable that the Zr_3Al^+ , Zr_4Al^- , Zr_5Al^+ , Zr_6Al^- and Zr_7Al clusters are more stable than their corresponding differently charged species judged by the fragmentation energies and the second-order difference energies. The HOMO-LUMO energy gaps indicate that the $AlZr$ cluster has the highest chemical activity, while the $AlZr_2^+$ cluster is the most inert in $Zr_nAl^{\pm m}$ clusters. Natural electron populations show that the electrons transfer from the Zr atoms to Al atom only in $Zr_4Al^{\pm m}$ clusters.

Acknowledgments

We gratefully acknowledge the project funded by the Priority Academic Program Development of Jiangsu Higher Education Institutions for partial financial support.

References

- Addicoat, M. A., Buntine, M. A., & Metha, G. F. (2007). BFW: A Density Functional for transition metal clusters. *J. Phys. Chem. A* *111*, 2625-2628. <http://dx.doi.org/10.1021/jp0677521>
- Alexandrova, A. N., Zhai, H. J., Wang, L. S., & Boldyrev, A. I. (2004). Molecular wheel B_8^{2-} as a new inorganic ligand. photoelectron spectroscopy and ab initio characterization of LiB_8^- . *Inorg. Chem.*, *43*, 3552-3554. <http://dx.doi.org/10.1021/ic049706a>
- Becke, A. D. (1993). Density-functional thermochemistry. III. The role of exchange, *J. Chem. Phys.*, *98*, 5648-5652.
- Carpenter, J. E., & Weinhold, F. (1988). Analysis of the geometry of the hydroxymethyl radical by the "different hybrids for different spins" natural bond orbital procedure. *J. Mol. Struct. (THEOCHEM)*, *169*, 41-62. [http://dx.doi.org/10.1016/0166-1280\(88\)80248-3](http://dx.doi.org/10.1016/0166-1280(88)80248-3)
- Doverstål, M., Karlsson, L., Lindgren, B., & Sassenberg, U. (1998). Resonant two-photon ionization spectroscopy studies of jet-cooled Zr_2 . *J. Phys. B: At. Mol. Opt. Phys.*, *31*, 795-803. <http://dx.doi.org/10.1088/0953-4075/31/4/025>
- Du, J. G., Sun, X. Y., & Jiang, G. (2010). Structures, chemical bonding, magnetisms of small Al-doped zirconium clusters. *Phys. Lett. A* *374*, 854-860. <http://dx.doi.org/10.1016/j.physleta.2009.12.009>
- Feng, X. J., & Luo, Y. H. (2007). Structure and stability of Al-doped boron clusters by the density-functional theory. *J. Phys. Chem. A*, *111*(12), 2420-2425. <http://dx.doi.org/10.1021/jp0656429>
- Frisch, M. J., Trucks, G. W., Schlegel, H. B., Scuseria, G. E., Robb, M. A., Cheeseman, J. R., ... Foresman, J. B. (2010). Gaussian 09. Gaussian, Inc., Wallingford.
- Fu, Z. W., Lemire, G. W., Bishea, G. A., & Morse, M. D. (1990). Spectroscopy and electronic structure of jet-cooled Al_2 . *J. Chem. Phys.*, *93*(12), 8420-8441. <http://dx.doi.org/10.1063/1.459280>
- Ge, G. X., Jing, Q., Cao, H. B., & Yan, H. X. (2012). Structural, electronic, and magnetic properties of MB_n ($M = Y, Zr, Nb, Mo, Tc, Ru, n \leq 8$) clusters. *J. Clust. Sci.*, *23*(2), 189-202. <http://dx.doi.org/10.1007/s10876-011-0419-x>
- Hay, P. J., & Wadt, W. R. (1985). Ab initio effective core potentials for molecular calculations. Potentials for K to Au including the outermost core orbitals. *J. Chem. Phys.*, *82*, 299-310. <http://dx.doi.org/10.1063/1.448975>

- Herry, D. J. (2012). Structures and stability of doped gallium nanoclusters. *J. Phys. Chem. C* 116 (46), 24814-24823. <http://dx.doi.org/10.1021/jp307555r>
- Hua, Y. W., Liu, Y. L., Jiang, G., Du, J. G., & Chen, J. (2013). Geometric transition and electronic properties of titanium-doped aluminum clusters: Al_nTi ($n = 2 - 24$). *J. Phys. Chem. A*, 117, 2590-2597. <http://dx.doi.org/10.1021/jp309629y>
- Lee, C., Yang, W. T., & Parr, R. G. (1988). Development of the Colle-Salvetti correlation-energy formula into a functional of the electron density. *Phys. Rev. B* 37, 785. <http://dx.doi.org/10.1103/physrevb.37.785>
- Lei, X. L. (2011). Geometrical and electronic properties of neutral and anionic Al_nB_m ($n + m = 13$) clusters. *J. Clust. Sci.*, 22, 159-172. <http://dx.doi.org/10.1007/s10876-011-0370-x>
- Lekka, C. E. (2010). Cu-Zr, and Cu-Zr-Al clusters: Bonding characteristics and mechanical properties. *J. Alloy. Compd.* 504, 190-193. <http://dx.doi.org/10.1016/j.jallcom.2010.02.067>
- Parr, R. G., & Zhou, Z. X. (1993). Absolute Hardness: Unifying concept for identifying shells and subshells in nuclei, atoms, molecules, and metallic clusters. *Acc. Chem. Res.* 26, 256-258. <http://dx.doi.org/10.1021/ar00029a005>
- Pearson, R. G. (2005). Chemical hardness and density functional theory. *J. Chem. Sci.*, 117(5), 369-377. <http://dx.doi.org/10.1007/BF02708340>
- Ramos-Castillo, C. M., Reveles, J. U., Zope, R. R., & de Coss, R. (2015). Palladium clusters supported on graphene monovacancies for hydrogen storage. *J. Phys. Chem. C*, 119(15), 8402-8409. <http://dx.doi.org/10.1021/acs.jpcc.5b02358>
- Reed, A. E., Curtiss, L. A., & Weinhold, F. (1988). Intermolecular interactions from a natural bond orbital, Donor-Acceptor Viewpoint. *Chem. Rev.*, 88(6), 899-926. <http://dx.doi.org/10.1021/cr00088a005>
- Schmidt, M., Kusche, R., Issendorff, B. V., & Haberland, H. (1998). Irregular variations in the melting point of size-selected atomic clusters. *Nature*, 393, 238-240. <http://dx.doi.org/10.1038/30415>
- Sengupta, T., Das, S., & Pal, S. (2016). Transition Metal Doped Aluminum Clusters: An Account of Spin. *J. Phys. Chem. C* 120, 10027-10040. <http://dx.doi.org/10.1021/acs.jpcc.6b00510>
- Sheng, X. F., Zhao, G. F., & Zhi, L. L. (2008). Evolution of small Zr clusters and dissociative chemisorption of H_2 on Zr clusters. *J. Phys. Chem. C* 112, 17828-17834. <http://dx.doi.org/10.1021/jp8072602>
- Suh, Y. J., Chae, J. W., Jang, H. D., & Cho, K. (2015). Role of chemical hardness in the adsorption of hexavalent chromium species onto metal oxide nanoparticles. *Chem. Eng. J.*, 273, 401-405. <http://dx.doi.org/10.1016/j.cej.2015.03.095>
- Tang, X., Bumüller, D., Lim, A., Schneider, J., Heiz, U., Ganteför, G., Fairbrother, D. H., & Bowen, K. H. (2014). Catalytic dehydration of 2-Propanol by Size-Selected $(WO_3)_n$ and $(MoO_3)_n$ metal oxide clusters. *J. Phys. Chem. C* 118(50), 29278-29286. <http://dx.doi.org/10.1021/jp505440g>
- Wang, C. C. (2006). Geometries and magnetisms of the Zr_n ($n = 2 - 8$) clusters: The density functional investigations. *J. Chem. Phys.*, 124, 194301. <http://dx.doi.org/10.1063/1.2200346>
- Wang, J., Liu, Y., & Lia, Y. C. (2010). Au@Sin: Growth behavior, stability and electronic structure. *Phys. Lett. A* 374(27), 2736-2742. <http://dx.doi.org/10.1016/j.physleta.2010.04.068>
- Wu, Y. Y., Xu, S. Y., Zhao, F. Q., & Ju, X. H. (2015). Adsorption and dissociation of H_2 on B_n and MgB_n ($n = 2 - 7$) clusters: A DFT investigation. *J. Clust. Sci.*, 26(3), 983-999. <http://dx.doi.org/10.1007/s10876-014-0791-4>
- Wu, Y. Y., Zhao, F. Q., & Ju, X. H. (2014). DFT study on structure and stability of $MgB_n^{\pm m}$ clusters. *Comput. Theor. Chem.*, 1027, 151-159. <http://dx.doi.org/10.1016/j.comptc.2013.11.001>
- Wu, Z. K., Gayathri, C., Gri, R. R., & Jin, R. (2009). Probing the structure and charge state of Glutathione-Capped $Au_{25}(SG)_{18}$ clusters by NMR and Mass Spectrometry. *J. Am. Chem. Soc.*, 131(18), 6535-6542. <http://dx.doi.org/10.1021/ja900386s>
- Yamazoe, S., Koyasu, K., & Tsukuda, T. (2014). Nonscalable Oxidation Catalysis of Gold Clusters. *Acc. Chem. Res.* 47(3), 816-824. <http://dx.doi.org/10.1021/ar400209a>
- Yang, C. L., Wang, M. S., Sun, M. Y., Wang, D. H., Ma, X. G., & Gong, Y. B. (2008). Dominant role of the interstitial 4d transition-metal in $TM@Zr^{Z}_{12}$ ($TM = Y-Cd$, $Z = 0, \pm 1$) icosahedral cages. *Chem. Phys. Lett.* 457, 49-53. <http://dx.doi.org/10.1016/j.cplett.2008.04.023>
- Yao, J. G., Wang, X. W., Wang, Y. X. (2008). A theoretical study on structural and electronic properties of Zr-doped B

clusters: ZrB_n ($n = 1-12$). *Chem. Phys.*, 351, 1-6. <http://dx.doi.org/10.1016/j.chemphys.2008.03.020>

Zhai, H. J., Kiran, B., Li, J., & Wang, L. S. (2003). Hydrocarbon analogues of boron clusters-planarity, aromaticity and antiaromaticity. *Nature Mater*, 2, 827-833. <http://dx.doi.org/10.1038/nmat1012>

Zhao, G. F., Sheng, X. F., Zhi, L. L., Sun, J. M., & Gu, Y. Z. (2009). Density-functional study of structural, electronic, and magnetic properties of the Zr_nCr ($n = 2-14$) clusters. *J. Mol. Struct. (THEOCHEM)*, 908, 40-46. <http://dx.doi.org/10.1016/j.theochem.2009.04.041>

Copyrights

Copyright for this article is retained by the author(s), with first publication rights granted to the journal.

This is an open-access article distributed under the terms and conditions of the Creative Commons Attribution license (<http://creativecommons.org/licenses/by/4.0/>).